ACS OMEGA

Open Access

http://pubs.acs.org/journal/acsodf

Article

Effects of Diamond Content on the Morphology and Compressive Properties of Porous Aluminum Composites

Bisma Parveez, Nur Ayuni Jamal,* Nur Izzah Nazurah, Abdul Aabid, and Muneer Baig

Cite This: *ACS Omega* 2024, 9, 36690−36698

Read Online

ACCESS | Metrics & More | Article Recommendations

ABSTRACT: Porous aluminum (Al) is popular due to its lightweight properties and impact energy absorption. However, it often has a lower mechanical strength than solid Al. To improve the performance, diamond reinforcement was introduced into the matrix. Further, addressing the challenge of interfacial bonding between Al and diamond, coated diamond with varying contents of 5, 10, 15, and 20 wt % was added to the porous Al alloy matrix via the powder metallurgy technique. The porosities were formed by using poly(methyl methacrylate) (30 wt %) as a space holder. The densities of the resultant porous composites ranged from 2.20 to 2.37 g/cm^3 and porosities ranged from 33 to 38% for 5−20 wt % diamond contents. Furthermore, the yield strength and plateau stress increased from 21.47 to 29.46 MPa and 14 to 20 MPa, respectively, up to 10 wt % diamond content but declined upon further addition. Similarly, the energy absorption capacity increased from 2.15 to 2.95 MJ/m^3 up to 10 wt % diamond content and thereafter decreased. Thus, the addition of coated diamond and alloying elements in Al strengthened the porous Al composites, making it suitable for applications requiring good compressive strength and energy absorption capacity.

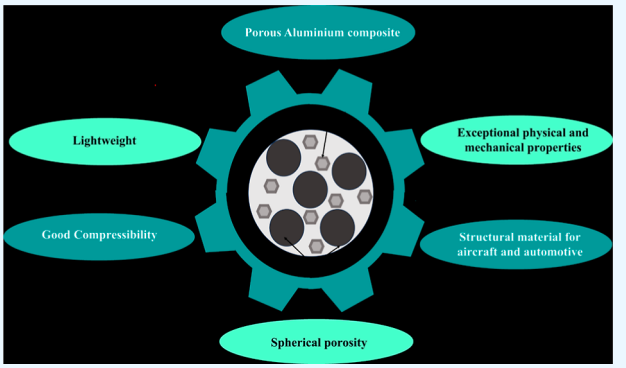

1. INTRODUCTION

The automotive industry requires lightweight materials with high energy absorption and sound insulation. Aluminum (Al)-based alloys and composites are highly studied for meeting such requirements due to their lightweight and high strength properties. Further reduction in their weight was possibly done by developing porous Al alloys and composites with higher impact energy absorbing capacities.[1,2] Porous Al, due to its lightweight properties, has the potential to reduce the total weight of a vehicle if employed as fillers in automotive parts, resulting in less fuel consumption and low carbon dioxide emissions to the environment, thereby reducing the carbon footprint. Furthermore, porous Al has high impact energy absorbing capacity, required in automotives to absorb energy during impact, thus preventing damage to the passengers as well as expensive car components. Despite its excellent properties, its porous structure gives it lower physical and mechanical properties than that of conventional solid Al. To improve their performance, high strength materials such as ceramics.[3−5] and carbonaceous reinforcements[6] have been added to porous Al. These reinforcements exhibited a strengthening effect in porous Al composites.

Diamond is one such carbonaceous reinforcement that is studied extensively for consideration as reinforcing materials due to its promising hardness property and thermal conductivity, which can extend the service life of the resultant material while delivering the strengthening effect simultaneously.[7] Although the expected results are promising, incorporating diamond in a porous Al matrix is difficult due to its poor wettability with a metal matrix. As a result, desirable interfacial bonding is not hard to achieve between the metal matrix and diamond, which otherwise is required in order to attain optimal properties of the resultant porous Al composite. One of the techniques to address the issue of poor interface bonding between diamond and Al is to coat the diamond particles with a metal layer. This metallic layer forms carbides at the interface, which are found to form chemical bonds with diamond and also combine with the Al matrix, thereby improving interfacial bonding. Various metallic coatings have been employed to improve the interface between diamond and Al such as molybdenum, tungsten, or titanium (Ti) coating.[8−11] However, Ti has been preferred because it not only reacts with diamond particles to form TiC but also reacts with the Al matrix to form a new phase. This carbide layer at the

Received: June 8, 2024
Revised: July 31, 2024
Accepted: August 2, 2024
Published: August 17, 2024

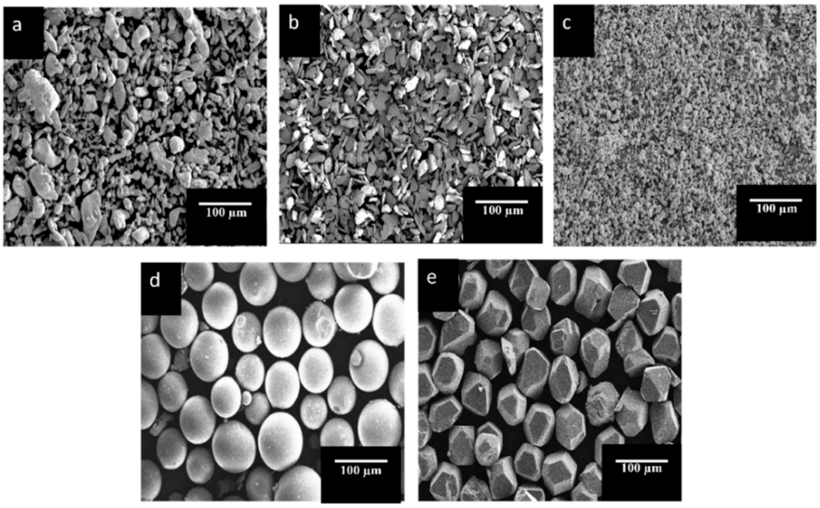

Figure 1. SEM micrographs of composite constituents: (a) Al, (b) Mg, (c) Sn, (d) PMMA particles, and (e) Ti-coated diamond.

diamond−metal interface prevents the reaction of carbon from diamond with the metal matrix, which can otherwise lead to formation of undesirable carbides (Al_4C_3). Moreover, the metallurgical bonding of coating metal with matrix material leads to improvement in the interfacial bonding between diamond particles and the metal matrix.[12,13]

Another technique applied to modify the interfacial bonding between diamond and Al matrixes in Al/diamond composites is matrix alloying. Matrix alloying is another technique for modifying the interfacial properties of diamond/aluminum composites. Alloying elements can improve the wettability between Al and diamond, resulting in a stable interface structure, as well as prevent excessive Al_4C_3 phase formation, which can negatively affect the properties.[14] Researchers have utilized materials such as Si, Mg, Sn, and B[15−17] as alloying elements. This method is also a cost-effective and efficient interface modification method.

Several fabrication processes have been employed to develop porous Al; however, to have better control over porosity and reinforcements distribution, the powder metallurgy method is mostly preferred.[18,19] The solid-state method allows easy control over the weight fraction of diamond and aluminum, and the lower fabrication temperature eliminates the formation of undesirable carbides (Al_4C_3) in the porous composites. Moreover, the porosities in such materials are tailored by employing space holders, which are added to the mixture and later removed during or after sintering. The space holder is meant to hold spaces in the green compacts that will eventually form pores on their decomposition or dissolution, resulting in the formation of a porous structure. Sodium chloride (NaCl), carbamide (ammonium bicarbonate), carbonate particles, and polymers such as poly(methyl methacrylate) (PMMA) are the commonly used space holders.[20−24] Except PMMA, all other space holders are leached out by carrying out the dissolution process after sintering; however, they are associated with issues like incomplete leaching, corrosion by salts, and additional dissolution process requirement. However, PMMA particles get decomposed al lower temperature during the sintering process, leaving almost no residue behind, and have the least reactivity with porous Al.[25,26] Further, they have good formability, and their spherical shape also contributes to significant improvement in the mechanical properties of porous materials.[7,27]

This study focused on investigating the microstructure, density, porosities, phase structure, and compressive properties of porous Al composites reinforced with varying Ti-coated diamond content fabricated via the powder metallurgy technique. The porosities were tailored using polymer (PMMA)-based space holders. The present work aims to provide new insights into enhancing the performance of porous Al composites that can benefit automotive industries in providing lightweight and safer structures.

2. EXPERIMENTAL PROCEDURE

2.1. Materials. The materials utilized in this study are Al, Mg, Sn, PMMA particles, and Ti-coated diamond, as shown in the scanning electron microscopy (SEM) images in Figure 1. The metallic powders (Al, Mg, and Sn) of purity and particle size, as mentioned in Table 1, were procured from Nova Scientific resources Malaysia Sdn Bhd. Varying contents of Ti-coated diamond particles as reinforcements and a fixed content (30 wt %) of PMMA particles as space holder particles were employed, as shown in Figure 1 (see Table 2).

Table 1. Particle Size of Composite Constituents

composite constituents	particle size (μm)	purity (%)
aluminum	75	99.5
magnesium	45	99.5
tin	10	99.5
PMMA	150	99.9
titanium-coated diamond	45	99.8

2.2. Methods. The methodology applied to fabricate porous Al composites was powder metallurgy, which involved

Table 2. Compressive Properties of Porous Al Composites with Varying Diamond Content

diamond content (%)	yield strength (MPa)	plateau stress (MPa)	energy absorption capability (MJ/m^3)
5	21.47	14	2.15
10	29.46	20	2.95
15	18.15	8	1.71
20	9.56	2.5	0.48

https://doi.org/10.1021/acsomega.4c05354
ACS Omega 2024, 9, 36690−36698

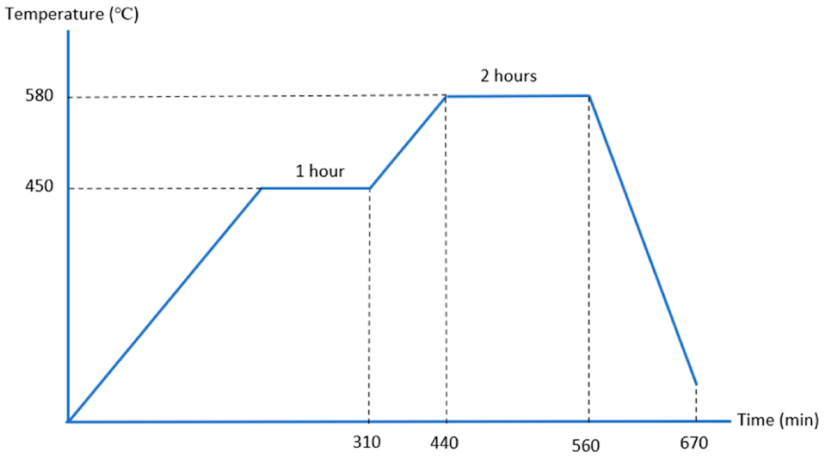

Figure 2. Sintering temperature vs sintering time graph.

mainly three stages: mixing, compaction, and sintering. The initial process of mixing was carried out in two steps: first, metallic powders of Al, Mg (2 wt %), and Sn (2 wt %) were mixed at a speed of 225 rpm for 12 h in a ball mill. Then, the metallic powder mixture was mixed with PMMA (30 wt %) particles and varying contents (5, 10, 15, and 20 wt %) of diamond particles at 800 rpm for 2 h in an orbital shaker. The resultant mixture was then compacted at a pressure of 250 MPa using a uniaxial hydraulic press. Then, the compacted samples were sintered in accordance with the graph of sintering temperature vs sintering time as shown in Figure 2.

The compacted samples were initially heated for 1 h at a temperature of 450 °C, which was set above the degradation temperature of PMMA, as illustrated by the thermal decomposition graph of PMMA particles in Figure 3. The

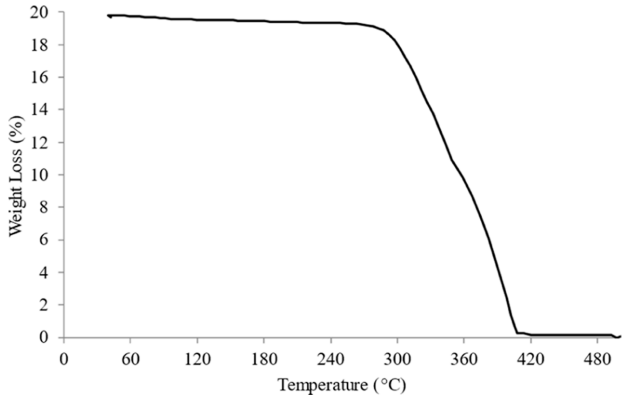

Figure 3. Degradation behavior of the PMMA space holder.

degradation of PMMA starts at 270 °C (T_s) and ends at 410 °C (T_f); thus, 450 °C was sufficient to decompose all PMMA particles required to obtain a desirable porous structure. Further, the sintering was carried out at 580 °C for 2 h in an argon atmosphere using a Carbolite tube furnace.

2.3. Characterization. The microstructure, densities, crystallinity, and compression behavior of the porous Al composite were observed. The density and porosity level of the samples were measured by applying the Archimedes principle. The morphology of the samples was analyzed using SEM (JEOL JSM-6300F). The X-ray diffraction (XRD) analysis was carried out using an X-ray diffractometer (PAN analytical empyrean 1032) operating at 40 kV and 40 mA in the 20−80° range. The compressive properties were measured using a universal testing machine (Shimadzu Autograph AGX 10 kN) at a crosshead speed of 0.5 mm/min and a compression load of 10 kN. The energy absorption capacity (W) of the resulting porous composites was calculated using the stress−strain curve using the following equation.[28]

$$W = \int_0^{\varepsilon} \sigma d\varepsilon \quad (1)$$

where σ and ε are the compressive stress and strain, respectively.

3. RESULTS AND DISCUSSION

3.1. Morphology. Figure 4 illustrates the homogeneous powder mixture without powder clustering. It demonstrates

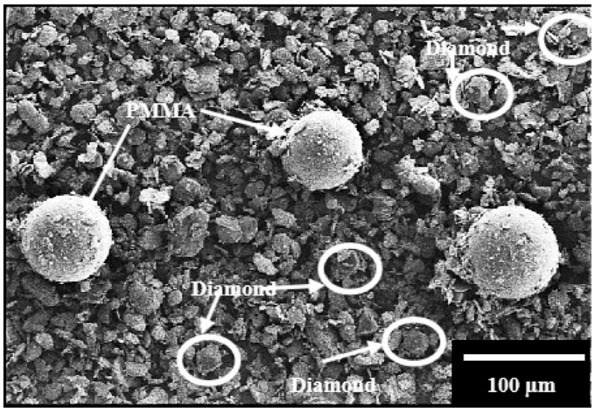

Figure 4. Morphology of the powder mixture.

that 12 h mixing time was sufficient to achieve a uniform powder mixture. All of the constituents were mixed to play a specific role in porous composite preparation. Tin was added to Al in order to enhance fluidity during sintering, while Mg powder improved the wettability of Al and also increased the segregation of Sn particles on the surface of Al particles.[29,30] Furthermore, spherical shaped PMMA particles were added to tailor spherical porosities in the resultant porous composites; however, PMMA has low affinity with metal powder. Thus, to ensure effective adhesion of PMMA with the metal matrix, CLE safe oil as the binder is mixed with PMMA particles, which makes their surface sticky for metal particles to adhere

https://doi.org/10.1021/acsomega.4c05354
ACS Omega 2024, 9, 36690−36698

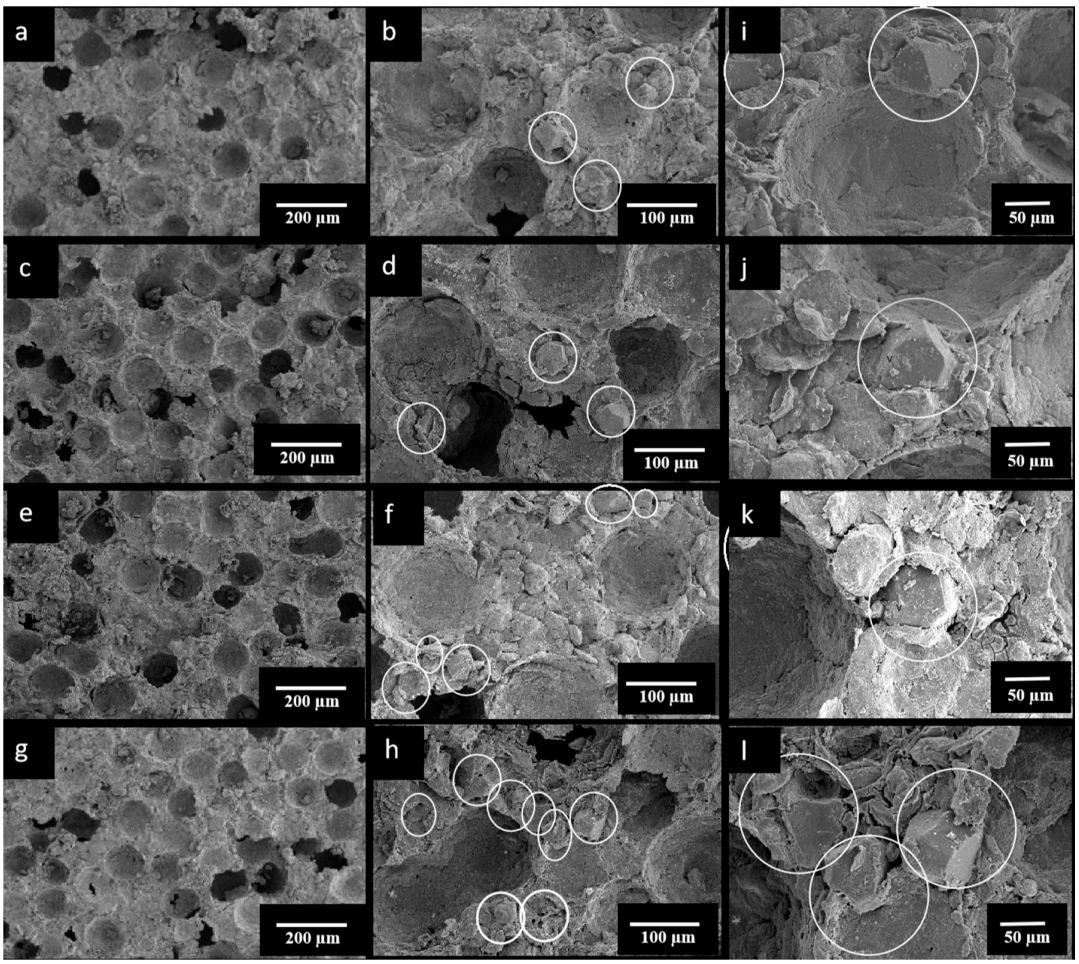

Figure 5. Morphology of porous Al composites at 200, 100, and 50 μm with [a,b,(i)] 5 wt %, (c,d,j) 10 wt %, (e,f,k) 15 wt %, and (g,h,l) 20 wt % diamond content.

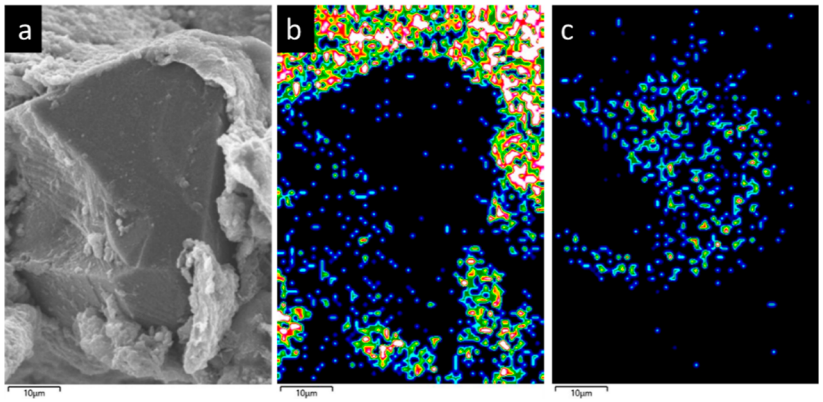

Figure 6. (a) Morphology and energy-dispersive X-ray area mapping on Ti-coated diamond particles in the porous Al composite, (b) with distribution of the Al alloy matrix (colored dots other than blue), and (c) Ti coating (blue color dots).

during mixing, followed by better bonding during compaction. As evident from Figure 4, PMMA particles were coated with the constituents of the powder mixture.

The morphology of porous Al composites with diamond contents of 5, 10, 15, and 20 wt % is shown in Figure 5a–l. As a result of removal of PMMA during sintering, the resultant porous Al exhibits a distinct closed macro-pore structure for each diamond content. Furthermore, these closed macro-pores exhibited a perfectly spherical shape that matches the initial morphology of PMMA particles. According to previous research, it is critical to make sure that the pore morphology replicates the morphology of the space holders in order to have a better control over pore shape and size for obtaining high-quality porous Al.[31−33] Furthermore, the shape and size of the space holders have a significant influence on the microstructure and mechanical properties of porous Al.[34] Similarly, it has been observed that the high strength and low elastic modulus of the resultant porous Al can be obtained by opting for a space

https://doi.org/10.1021/acsomega.4c05354
ACS Omega 2024, 9, 36690−36698

holder material with desirable morphology.[32] Furthermore, the shape of the space holders also affects the properties of the porous composites. Especially, spherical shaped space holders demonstrate higher compressive strength by virtue of the spherical pores being formed when compared to those with irregular shaped pores.[35] As is evident from Figure 5, pores replicated the spherical shape of PMMA particles (Figure 1d).

As illustrated in Figure 5i,j, for 5 and 10 wt % diamond contents, the Al matrix adheres and bonds well with the diamond particles. Moreover, using Ti-coated diamond as a reinforcement improved the bonding at the interface of the Al alloy matrix and diamond particles. Figure 6 depicts the distribution of the Al alloy matrix, shown by multicolored dots (Figure 6b), and Ti coating, shown by blue dots near the diamond particles in the porous composite. Since Ti atoms get accumulated on the surface of diamond particles, few of them diffuse into the Al alloy matrix. The presence of Al near or overlapping the Ti region on the diamond surface (Figure 6c) suggests a bond between the Al alloy matrix and the Ti-coated diamond particles. Other studies also revealed the function of coating on diamond particles improving the interfacial bonding between the metal matrix and diamond particles, significantly improving the wetting property between the metal matrix and diamond particles.[36,37] However, due to the presence of TiC on the surface of diamond particles, AlC can also form and impair the bonding at some contacts. But, overall, the way the Al matrix alloy is spread over the diamond particle proves that the adhesion has been improved to some extent by employing coated diamond as compared to that for the porous Al reinforced with uncoated diamond employed in one of our studies.[16]

However, as the diamond content increases, the diamond particle is not completely covered by the Al matrix, as shown in Figure 5f,h for 15 and 20 wt % diamond contents. The gaps and pores are present between the Al alloy matrix and the diamond particle, indicating poor interfacial bonding between them. These gaps and pores are formed as a result of the agglomeration of diamond particles, as evident from Figure 5f,h, which leads to ineffective sintering of the porous Al specimen, thereby resulting in leaving gaps at the interfaces. In addition, at higher diamond content, due to the absence of enough Al alloy matrix required to bind the diamond particles in the porous Al composites, weak interfacial bonding occurred.

3.2. Density and Porosity. The sintered densities of porous Al reinforced with diamond particles (5, 10, 15, and 20 wt %) are shown in Figure 7. The densities were found to increase from 2.2 to 2.37 g/cm^3 with the increase in the diamond content from 5 to 20 wt %, respectively, a high-density reinforcement. The diamond particles are denser than the Al alloy matrix; although the theoretical density of the porous composites increases, their bulk density also increases. In addition, the porosities of Ti-coated diamond-reinforced porous Al composites were found to increase from 33 to 38% with the increase in the diamond content from 5 to 20 wt %, respectively. Since the tailored porosity should be only 30% as per the addition of 30 wt % of PMMA space holder particles, the increased values of porosities are due to the undesirable pores and gaps formed during the sintering process, as shown in Figure 5. In addition, higher porosity levels were attained for porous composites with higher wt % of diamond particles as a result of their agglomeration tendency at higher content, resulting in gaps between adjacent diamond particles, and also

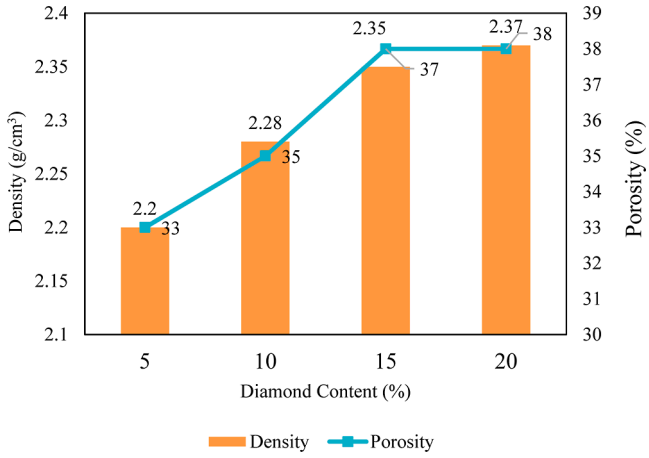

Figure 7. Sintered densities and porosities of diamond-reinforced composites.

due to insufficient availability of the Al alloy matrix to fill the gaps, as evident from Figure 5f,h.

3.3. X-ray Diffraction. Figure 8 shows the XRD pattern of the final powder mixture consisting of Al, Mg, Sn, PMMA, and Ti-coated diamond. The main diffraction peaks were observed for Al for (111), (200), (220), and (311) planes at 38.47, 44.74, 65.14, and 78.23°, respectively. Diamond peaks at 43.72 and 74.90°, α-Ti peaks at 37.20 and 40.50°, and titanium carbide (δ-TiC) peaks at 35.10, 42.20, and 62.50° confirm the presence of Ti coating on the as-received diamond and imply successful TiC formation during the coating process.[37] The diffraction peaks of diamond, α-Ti, and δ-TiC indicated their formations during the application of coating, where carbon atoms of diamond diffuse into the metallic coating (Ti), thereby occupying an octahedral interstitial position in the Ti crystal lattice, resulting in the formation of a δ−TiC transition layer. Its metallurgy combines with diamond. Then, on addition of coated diamond particles to the Al alloy matrix, the α-Ti layer present on the surface of coated diamond wets the Al matrix.[38]

Figure 9a−d demonstrates the XRD patterns of porous Al composites with 5, 10, 15, and 20 wt % diamond contents, respectively. Apart from the four typical Al peaks at 38.5, 44.7, 65.1, and 78.2°, representing (111), (200), (220), and (311) planes, respectively, the low-intensity peaks of diamond were also detected at 43.9 and 75.29°. However, insignificant intensities of the peaks of aluminum carbide (Al_4C_3) were also detected in the range of θ = 20°−80°, which may be due to the reaction of the few carbides in coating with the Al alloy matrix. But, overall, the fabrication at low sintering temperature and the presence of coating further inhibited its formation. Similar results for XRD have been attained by using B4C-coated diamond and Ti-coated diamond as reinforcements in Al composites.[37,39] Also, from Figure 9a−d, it can be seen that the porous Al composites exhibited higher and sharper peaks with increasing diamond content, implying crystalline phases of Al and diamond particles and thus indicating the effective sintering of porous composites.[40]

3.4. Compressive Behavior. Figure 10 shows the stress−strain curves obtained on compression loading of porous Al composites with 5, 10, 15, and 20 wt % diamond content. The stress−strain curves show all three regions: elastic, plateau, and densification;[41,42] the first stage of deformation is the linear elastic region, followed by a constant stress region over a wide

https://doi.org/10.1021/acsomega.4c05354
ACS Omega 2024, 9, 36690−36698

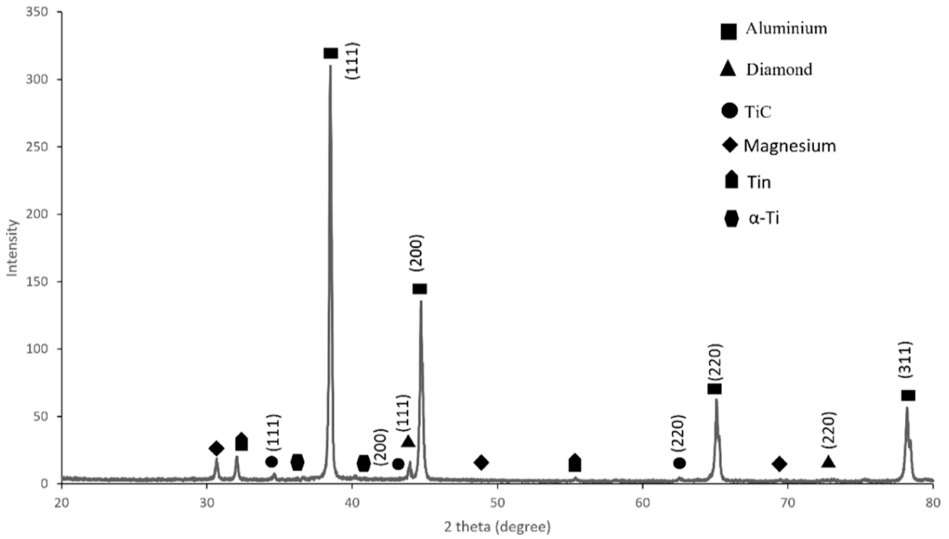

Figure 8. XRD analysis of the powder mixture.

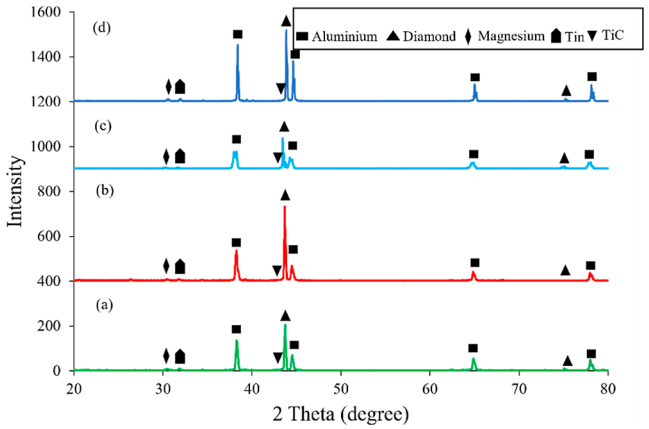

Figure 9. XRD patterns of porous Al composites with (a) 5 wt %, (b) 10 wt %, (c) 15 wt %, and (d) 20 wt % diamond content.

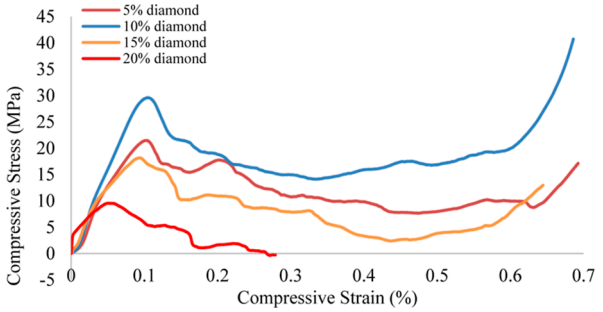

Figure 10. Compressive stress−strain curve of porous Al composites with varying diamond content.

range of strains, called as the plateau region, and, finally, a densification region where stress increases rapidly due to cell wall collapse. The stress−strain curves exhibit brittle behavior with severe variations over the plateau region. Other studies using ceramic and carbon nanotubes as reinforcements have also observed similar fluctuations.[43−45]

The yield strength and plateau stress of porous Al composites increase with an increase in diamond content up to 10 wt %, followed by a decrease on further addition, and the highest yield strength of 29.46 MPa and plateau stress of 20 MPa were obtained for porous Al composites with 10 wt % diamond content. The higher values are due to the uniformity of the pore structure and the presence of better bonded diamond particles in the Al alloy matrix, thereby offering effective load transfer and thus improving its yield strength and plateau stress on the application of load. However, the declination on further addition of diamond particles is due to the poor wettability of diamond with the Al alloy matrix and also due to agglomeration occurring at higher diamond content, resulting in the formation of undesirable gaps and porosities, as confirmed by Figure 5f,h and increased porosity values in Figure 6.

3.5. Energy Absorption Characteristics. The energy absorption capability of the porous composites was evaluated by calculating the area under the curve of the plateau region using eq 1. As evident from Figure 9, the energy absorption capacity increases on addition of diamond content up to 10 wt % and then declines on further inclusion. The maximum value of 2.95 Mj/m^3 was attained at 10 wt % diamond content. The increased value of energy absorption capacity is due to the ductile fracture mode resulting from better bonded porous composites with good interfacial bonding between Ti-coated diamond and the Al alloy matrix.[39] On the other hand, the energy absorption capacity values declined on further increase in diamond particles content, similarly to plateau stress.[25] At higher diamond particle content, the presence of an insufficient Al alloy matrix for wetting of diamond particles forms gaps and pores in the cell walls, leading to poor mechanical bonding between the Al alloy matrix and diamond particles. It regulates the collapse of cell walls by dropping the bending deformation resistance, thus reducing their capability to resist deformation and dissipate impact energy.[40]

The compressive properties of porous Al composites if compared to other studies, as shown in Table 3, show better plateau stress values than others. However, the energy absorption values of the present work are lower, and this can be attributed to the challenges in getting good wettability of diamond particles in the Al matrix. Still, the energy absorption of the porous Al composites reinforced with coated and uncoated diamond particles in previous studies exhibited lower values than those in the present work, thereby revealing the

https://doi.org/10.1021/acsomega.4c05354
ACS Omega 2024, 9, 36690−36698

Table 3. Comparison of Compressive Properties in Other Studies with Those in the Present Work

composition	plateau stress (MPa)	energy absorption capacity (Mj/m^3)	references
Al/$MgAl_2O_4$	18.7	17.5	46
A356/SiC	12	8	47
$AlSi_9Mg$/SiCp	15	12	48
AlMgSn/diamond	7.50	1.7	16
AlMgSn/Ti-coated diamond	9.96	1.7	49
AlMgSn/Ti-coated diamond	**20**	**2.95**	**(Present work)**

improvement in the development of Ti-coated diamond-reinforced Al composites.

3.6. Deformation of Porous Al Composites. The deformation of porous composites occurs in a linear elastic manner due to cell wall bending, as shown in Figure 11, and

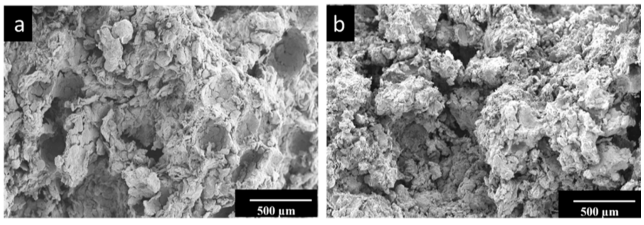

Figure 11. Deformation pattern of porous Al composites at (a) 10 and (b) 15 wt % diamond contents.

this elastic limit increases with diamond particle content, as evident from Figure 10. Since diamond has higher strength, it acts as a rigid body, and on application of the load, elastic deformation of the Al alloy matrix takes place. However, the duration of the elastic deformation period is brief due to the presence of diamond particles, which generate a considerable stress field in the Al alloy matrix. When the stress reaches higher than the yielding stress of Al, the occurrence of dislocations takes place. These dislocations cause the Al alloy matrix to deform plastically. As a result of the discrepancy in deformation between diamond rigid particles and the plastically deforming Al alloy matrix, strong strain gradients are formed in the Al alloy matrix.[50] These gradients do not allow dislocations to move smoothly in the Al matrix due to the presence of intensive triaxial stress constraint caused by the concentration of diamond particles around them. Additionally, the Al matrix shows a noticeable strain hardening effect. This effect stays until the dislocation movements get exhausted. Then, in order to relax stress concentration continuously, the Al matrix undergoes viscoelastic deformation, resulting in the development of voids and microcracks. On further increases in load, the cell walls start collapsing due to the voids and microcracks in the walls. Collapse begins at the yield strength of porous Al composites and advances at roughly a constant load, resulting in plateau stress, continuing until the opposing cell walls touch and meet, causing densification and a rapid increase in compressive stress. Finally, the damage extends quickly on reaching a significant size, resulting in abrupt fracture of the composites. The fracture mode was found to be ductile in porous composites with diamond content up to 10 wt %, and beyond this, due to higher voids and microcrack formations, it is more like brittle, as evident from Figure 11.

4. CONCLUSIONS

Porous Al composites of varying diamond contents (5, 10, 15, and 20 wt %) were developed via a powder metallurgy technique. The porosities were created using a fixed content (30 wt %) of PMMA particles. The effects of different diamond contents on the microstructure, densities, porosities, compressive properties, and deformation behavior of porous Al composites were systematically examined. The important findings are summarized as follows.

1. The porous Al composites had a closed macro-pore structure and uniformly distributed diamond reinforcement. The macro-pores resembled the spherical shape and size of PMMA particles. Morphological analysis of the porous Al composite showed strong interfacial bonding between the matrix and Ti-coated diamond up to 10 wt % diamond content. However, higher diamond contents (15 and 20 wt %) demonstrated pores and gaps at the interfaces.
2. XRD patterns of the porous Al composite with varying diamond content revealed peaks primarily composed of Al and diamond. These peaks became higher and sharper with the increase in diamond content. It indicated an increase in the crystalline phase of Al and diamond, thus implying an effective sintering process. Additional peaks of α-Ti and δ-TiC suggested the efficient coating of Ti on the surface of diamond particles.
3. Densities of porous Al composites increased from 2.20 to 2.37 g/cm^3 and the porosity level increased from 33 to 38% as the diamond content increased from 5 to 20%. Despite the addition of a fixed content (30 wt %) of PMMA as a space holder, increased porosities are caused by the presence of microporosities and gaps in the microstructure, especially in porous composites with higher diamond contents (15 and 20 wt %).
4. Diamond content affects the compressive behavior of porous Al composites. The yield strength, plateau stress, and energy absorption capacity initially increased up to 10 wt %, after which they decreased, and the highest values of 29.46 MPa, 20 MPa, and 2.95 MJ/m^3, respectively, were recorded for 10 wt % diamond content.
5. In this study, the optimum diamond content that improves the performance of porous Al composites in terms of density, porosity, yield strength, and energy absorption capacity was 10 wt % as it demonstrated a good combination of properties.

This work aimed to overcome the challenges of effectively utilizing diamond particles as reinforcements and improving their wettability in porous Al composites. Further investigation is required under different processing conditions by employing different processing techniques and techniques to obtain better interfacial bonding between the metal matrix and diamond particles for exploring their strengthening effects on the porous composites for lightweight and high-strength applications.

AUTHOR INFORMATION

Corresponding Author

Nur Ayuni Jamal − *Department of Manufacturing and Materials Engineering, Kulliyyah of Engineering, International Islamic University Malaysia, Kuala Lumpur 53100, Malaysia*; Email: ayuni_jamal@iium.edu.my

https://doi.org/10.1021/acsomega.4c05354
ACS Omega 2024, 9, 36690−36698

Authors

Bisma Parveez − *Department of Manufacturing and Materials Engineering, Kulliyyah of Engineering, International Islamic University Malaysia, Kuala Lumpur 53100, Malaysia;* orcid.org/0000-0003-1748-7989

Nur Izzah Nazurah − *Department of Manufacturing and Materials Engineering, Kulliyyah of Engineering, International Islamic University Malaysia, Kuala Lumpur 53100, Malaysia*

Abdul Aabid − *Department of Engineering Management, College of Engineering, Prince Sultan University, Riyadh 11586, Saudi Arabia*

Muneer Baig − *Department of Engineering Management, College of Engineering, Prince Sultan University, Riyadh 11586, Saudi Arabia*

Complete contact information is available at: https://pubs.acs.org/10.1021/acsomega.4c05354

Author Contributions

Conceptualization and supervision, N.A.J.; writing—original draft, review, and editing, B.P.; data collection, N.A.N.; validation, A.A.; and funding acquisition, M.B. All authors have read and agreed to the published version of the manuscript.

Funding

This research was supported by the Ministry of Higher Education (MOHE) of Malaysia and International Islamic University Malaysia (IIUM) (FRGS/1/2019/TK08/UIAM/02/5).

Notes

The authors declare no competing financial interest.

■ ACKNOWLEDGMENTS

This research was supported by the Structures and Materials (S&M) Research Lab of Prince Sultan University, and the authors acknowledge the Prince Sultan university for paying the article processing charges (APC).

■ REFERENCES

(1) Fleck, N. *Metal Foams: A Design Guide*; Elsevier, 2016, vol *3069*, pp 264..

(2) Goel, M. D.; Matsagar, V. A.; Marburg, S.; Gupta, A. K. Comparative Performance of Stiffened Sandwich Foam Panels under Impulsive Loading. *J. Perform. Constr. Facil.* **2013**, *27* (5), 540−549.

(3) Atturan, U. A.; Nandam, S. H.; Murty, B. S.; Sankaran, S. Processing and Characterization of In-Situ TiB2 Stabilized Closed Cell Aluminium Alloy Composite Foams. *Mater. Des.* **2016**, *101*, 245−253.

(4) Zhiqiang, G.; Donghui, M.; Xiaoguang, Y.; Xue, D. Effect of Mg Addition on the Foaming Behaviour of AlSi7 Based Alloy Prepared by Powder Metallurgy Method. *Xiyou Jinshu Cailiao Yu Gongcheng/Rare Met. Mater. Eng.* **2016**, *45* (12), 3068−3073.

(5) Das, S.; Rajak, D. K.; Khanna, S.; Mondal, D. P. Energy Absorption Behavior of Al-SiC-Graphene Composite Foam under a High Strain Rate. *Materials* **2020**, *13* (3), 783.

(6) Maiorano, L. P.; Castillo, R.; Molina, J. M. Al/Gf Composite Foams with SiC-Engineered Interfaces for the next Generation of Active Heat Dissipation Materials. *Compos. Part A Appl. Sci. Manuf.* **2023**, *166*, 107367.

(7) Parveez, B.; Jamal, N. A.; Aabid, A.; Baig, M. Microstructure and Strengthening Effect of Coated Diamond Particles on the Porous Aluminum Composites. *Materials (Basel).* **2023**, *16* (8), 3240−3312.

(8) Ukhina, A. V.; Bokhonov, B. B.; Dudina, D. V. Selective Deposition of Mo2C-Containing Coatings on {100} Facets of Synthetic Diamond Crystals. *Int. J. Mol. Sci.* **2022**, *23* (15), 8511.

(9) Damanik, F. S.; Damanik, M. S. F.; Lange, P. G. Effect of Nickel Coated of Carbon Fiber on Distribution of Carbon Fiber Reinforced Aluminium (AlSi7) Foam Composite by Powder Metallurgy. *Int. Conf. Innov. Technol.* **2019**, *1381*, 9−13.

(10) Chen, M.; Liu, B.; Ji, Z.; Jia, C.; Wu, Q.; Liu, Z. Mechanical Properties and Damping Properties of Carbon Nanotube-Reinforced Foam Aluminum with Small Aperture. *J. Mater. Res.* **2020**, *35* (19), 2567−2574.

(11) Zhang, C.; Wang, R.; Cai, Z.; Peng, C.; Wang, N. Low-Temperature Densification of Diamond/Cu Composite Prepared from Dual-Layer Coated Diamond Particles. *J. Mater. Sci. Mater. Electron.* **2015**, *26* (1), 185−190.

(12) Che, Z.; Wang, Q.; Wang, L.; Li, J.; Zhang, H.; Zhang, Y.; Wang, X.; Wang, J.; Kim, M. J. Interfacial Structure Evolution of Ti-Coated Diamond Particle Reinforced Al Matrix Composite Produced by Gas Pressure Infiltration. *Compos. Part B Eng.* **2017**, *113*, 285−290.

(13) Yang, W.; Peng, K.; Zhu, J.; Li, D.; Zhou, L. Enhanced Thermal Conductivity and Stability of Diamond/Aluminum Composite by Introduction of Carbide Interface Layer. *Diam. Relat. Mater.* **2014**, *46*, 35−41.

(14) B.Novak, K.; Tschope, A. P. R.; T, G. Fundamentals of Aluminium Carbide Formation. *Light Met.* **2012**, No. 2, 1−1407.

(15) Jiao, Z.; Kang, H.; Zhou, B.; Kang, A.; Wang, X.; Li, H.; Yu, Z.; Ma, L.; Zhou, K.; Wei, Q. Research Progress of Diamond/Aluminum Composite Interface Design. *Funct. Diam.* **2022**, *2* (1), 25−39.

(16) Parveez, B.; Jamal, N. A.; Raeez, M. Investigation of Morphology and Compressive Properties of Diamond Reinforced Porous Aluminium Composites. *Asian J. Fundam. Appl. Sci.* **2023**, *4* (1), 12−17.

(17) Parveez, B.; Jamal, N. A.; Anuar, H.; Ahmad, Y.; Aabid, A.; Baig, M. Microstructure and Mechanical Properties of Metal Foams Fabricated via Melt Foaming and Powder Metallurgy Technique: A Review. *Materials* **2022**, *15*, 5302.

(18) Yang, X.; Hu, Q.; Li, W.; Song, H.; Zou, T.; Zong, R.; Sha, J.; He, C.; Zhao, N. Compression-Compression Fatigue Performance of Aluminium Matrix Composite Foams Reinforced by Carbon Nanotubes. *Fatigue Fract. Eng. Mater. Struct.* **2020**, *43* (4), 744−756.

(19) Duarte, I.; Ventura, E.; Olhero, S.; Ferreira, J. M. F. A Novel Approach to Prepare Aluminium-Alloy Foams Reinforced by Carbon-Nanotubes. *Mater. Lett.* **2015**, *160*, 162−166.

(20) Jiang, B.; Wang, Z.; Zhao, N. Effect of Pore Size and Relative Density on the Mechanical Properties of Open Cell Aluminum Foams. *Scr. Mater.* **2007**, *56* (2), 169−172.

(21) Mohd Razali, R. N.; Abdullah, B.; Muhammad Hussain, I.; Ahmad, U. K.; Idham, M. F.; Ramli, A. Mechanical Properties of Aluminium Foam by Conventional Casting Combined with NaCL Space Holder. *Appl. Mech. Mater.* **2013**, *393*, 156−160.

(22) Yang, X.; Hu, Q.; Du, J.; Song, H.; Zou, T.; Sha, J.; He, C.; Zhao, N. Compression Fatigue Properties of Open-Cell Aluminum Foams Fabricated by Space-Holder Method. *Int. J. Fatigue* **2019**, *121*, 272−280.

(23) Yang, K.; Yang, X.; He, C.; Liu, E.; Shi, C.; Ma, L.; Li, Q.; Li, J.; Zhao, N. Damping Characteristics of Al Matrix Composite Foams Reinforced by In-Situ Grown Carbon Nanotubes. *Mater. Lett.* **2017**, *209*, 68−70.

(24) Parveez, B.; Jamal, N. A.; Maleque, M. A.; Rozhan, A. N.; Aabid, A.; Baig, M. Optimizing the Compressive Properties of Porous Aluminum Composites by Varying Diamond Content, Space Holder Size and Content. *Materials* **2023**, *16* (3), 921.

(25) Jamal, N. A.; Tan, A. W.; Yusof, F.; Katsuyoshi, K.; Hisashi, I.; Singh, S.; Anuar, H. Fabrication and Compressive Properties of Low to Medium Porosity Closed-Cell Porous Aluminum Using PMMA Space Holder Technique. *Materials* **2016**, *9* (4), 254.

(26) Tan, P. P.; Mohamad, H.; Anasyida, A. S. Properties of Porous Magnesium Using Polymethyl Methacrylate (PMMA) as a Space Holder. *J. Phys. Conf. Ser.* **2018**, *1082* (1), 012063−012066.

(27) Shahzeydi, M. H.; Parvanian, A. M.; Panjepour, M. The Distribution and Mechanism of Pore Formation in Copper Foams Fabricated by Lost Carbonate Sintering Method. *Mater. Charact.* **2016**, *111*, 21−30.
(28) Wang, H.; Su, M.; Hao, H. Compressive Properties and Energy Absorption Behavior of Mg17Al12/Al Ordered Structure Composites. *Compos. Part B Eng.* **2021**, *210* (2), 108688.
(29) Showaiter, N.; Youseffi, M. Compaction, Sintering and Mechanical Properties of Elemental 6061 Al Powder with and without Sintering Aids. *Mater. Des.* **2008**, *29* (4), 752−762.
(30) Jamal, N.; Tan, A.; Yusof, F.; Katsuyoshi, K.; Hisashi, I.; Singh, S.; Anuar, H. Fabrication and Compressive Properties of Low to Medium Porosity Closed-Cell Porous Aluminum Using PMMA Space Holder Technique. *Materials* **2016**, *9*, 254.
(31) Awad, M.; Hassan, N. M.; Kannan, S. Mechanical Properties of Melt Infiltration and Powder Metallurgy Fabricated Aluminum Metal Matrix Composite. *Proc. Inst. Mech. Eng. Part B J. Eng. Manuf.* **2021**, *235* (13), 2093−2107.
(32) Lee, B.; Lee, T.; Lee, Y.; Lee, D. J.; Jeong, J.; Yuh, J.; Oh, S. H.; Kim, H. S.; Lee, C. S. Space-Holder Effect on Designing Pore Structure and Determining Mechanical Properties in Porous Titanium. *Mater. Des.* **2014**, *57*, 712−718.
(33) Michailidis, N.; Tsouknidas, A.; Lefebvre, L. P.; Hipke, T.; Kanetake, N. Production, Characterization, and Applications of Porous Materials. *Adv. Mater. Sci. Eng.* **2014**, *2014*, 1−2.
(34) Khamsuk, S.; Choosakull, K.; Wanwong, P. Effect of Space Holder Size on the Porous High Purity Aluminum Property. *Key Eng. Mater.* **2020**, *846*, 93−98.
(35) Bekoz, N.; Oktay, E. Effects of Carbamide Shape and Content on Processing and Properties of Steel Foams. *J. Mater. Process. Technol.* **2012**, *212* (10), 2109−2116.
(36) Liang, X.; Jia, C.; Chu, K.; Chen, H.; Nie, J.; Gao, W. Thermal Conductivity and Microstructure of Al/Diamond Composites with Ti-Coated Diamond Particles Consolidated by Spark Plasma Sintering. *J. Compos. Mater.* **2012**, *46* (9), 1127−1136.
(37) Bo, Y. A.; Yu, J. K.; Chuang, C. H. Microstructure and Thermal Expansion of Ti Coated Diamond/Al Composites. *Trans. Nonferrous Met. Soc. China* **2009**, *19* (5), 1167−1173.
(38) Zhang, Y.; Wang, X.; Jiang, S.; Wu, J. Thermo-Physical Properties of Ti-Coated Diamond/Al Composites Prepared by Pressure Infiltration. *Mater. Sci. Forum* **2010**, *654*−*656*, 2572−2575.
(39) Sun, Y.; Zhang, C.; He, L.; Meng, Q.; Liu, B. C.; Gao, K.; Wu, J. Enhanced Bending Strength and Thermal Conductivity in Diamond/Al Composites with B4C Coating. *Sci. Rep.* **2018**, *8* (1), 11104−11112.
(40) Chung, C. Y.; Chu, C. H.; Lee, M. T.; Lin, C. M.; Lin, S. J. Effect of Titanium Addition on the Thermal Properties of Diamond/Cu-Ti Composites Fabricated by Pressureless Liquid-Phase Sintering Technique. *Sci. World J.* **2014**, *2014*, 1−7.
(41) Sahu, S.; Goel, M. D.; Mondal, D. P.; Das, S. High Temperature Compressive Deformation Behavior of ZA27-SiC Foam. *Mater. Sci. Eng., A* **2014**, *607*, 162−172.
(42) Aly, M. S. Behavior of Closed Cell Aluminium Foams upon Compressive Testing at Elevated Temperatures: Experimental Results. *Mater. Lett.* **2007**, *61* (14−15), 3138−3141.
(43) Mondal, D. P.; Goel, M. D.; Das, S. Effect of Strain Rate and Relative Density on Compressive Deformation Behaviour of Closed Cell Aluminum-Fly Ash Composite Foam. *Mater. Des.* **2009**, *30* (4), 1268−1274.
(44) Hakamada, M.; Nomura, T.; Yamada, Y.; Chino, Y.; Hosokawa, H.; Nakajima, T.; Chen, Y.; Kusuda, H.; Mabuchi, M. Compressive Properties at Elevated Temperatures of Porous Aluminum Processed by the Spacer Method. *J. Mater. Res.* **2005**, *20* (12), 3385−3390.
(45) Yang, K.; Yang, X.; Liu, E.; Shi, C.; Ma, L.; He, C.; Li, Q.; Li, J.; Zhao, N. Elevated Temperature Compressive Properties and Energy Absorption Response of In-Situ Grown CNT-Reinforced Al Composite Foams. *Mater. Sci. Eng., A* **2017**, *690*, 294−302.
(46) Guo, C.; Zou, T.; Shi, C.; Yang, X.; Zhao, N.; Liu, E.; He, C. Compressive Properties and Energy Absorption of Aluminum Composite Foams Reinforced by In-Situ Generated MgAl2O4 Whiskers. *Mater. Sci. Eng., A* **2015**, *645*, 1−7.
(47) Ravi Kumar, N. V.; Ramachandra Rao, N.; Gokhale, A. A. Effect of SiC Particle Content on Foaming and Mechanical Properties of Remelted and Diluted A356/SiC Composite. *Mater. Sci. Eng., A* **2014**, *598*, 343−349.
(48) Luo, Y.; Yu, S.; Liu, J.; Zhu, X.; Luo, Y. Compressive Property and Energy Absorption Characteristic of Open-Cell SiCp/AlSi9Mg Composite Foams. *J. Alloys Compd.* **2010**, *499* (2), 227−230.
(49) Parveez, B.; Jamal, N. A.; Raeez, M. Effect of Uncoated and Coated Diamond on the Compressive Properties of Porous Aluminium Composites: Auswirkung von Unbeschichtetem Und Beschichtetem Diamant Auf Die Druckeigenschaften von Porösen Aluminiumverbundwerkstoffen. *Materwiss. Werksttech.* **2023**, *54* (9), 1114−1121.
(50) Lee, W. M.; Zikry, M. A. Modeling the Interfacial Plastic Strain Incompatibilities Associated with Dispersed Particles in High Strength Aluminum Alloys. *Acta Mater.* **2012**, *60* (4), 1669−1679.

https://doi.org/10.1021/acsomega.4c05354
ACS Omega 2024, 9, 36690−36698